Tribology International 149 (2020) 105613

Contents lists available at ScienceDirect

Tribology International

journal homepage: www.elsevier.com/locate/triboint

Effect of laser surface texturing on friction behaviour in elastohydrodynamically lubricated point contacts under different sliding-rolling conditions

G. Boidi[a,*], I.S. Tertuliano[a], F.J. Profito[a], W. de Rossi[b], I.F. Machado[a]

[a] Escola Politécnica, University of São Paulo, São Paulo, Brazil
[b] Nuclear and Energy Research Institute – IPEN, São Paulo, Brazil

ABSTRACT

The Laser Surface Texturing (LST) technique has been largely investigated to improve the tribological performance of lubricated contacts. The present contribution is aimed at scrutinizing the influence of three texture configurations fabricated by LST on the tribological performance of elastohydrodynamic (EHD) point contacts under different slide-to-roll ratios (SRR), entrainment velocities and inlet temperatures. Friction experiments were conducted through a series of ball-on-disk tests in the MTM-2 (Mini-Traction Machine) tribometer. Main results showed that the texture configurations promoted significant effects under boundary and mixed lubrication conditions, and also affected the full-film EHD regime at higher temperatures. Furthermore, the tribological performance of textured samples was strongly related to the texture depth. Shallower texture designs (~0.5 μm) reduced friction compared to untextured material, whereas deeper features (> 1 μm) generally led to detrimental results. In general, dimples configuration decreased the lift-off speed and promoted full-film EHD conditions for a larger range of speeds, whereas radial curved grooves yielded to friction reduction under mixed lubrication conditions, moving the transition from boundary to mixed regimes to lower speeds, especially for intermediate lubricant viscosity.

1. Introduction

The reduction of pollution caused by gas emissions derived from transportation systems and industrial applications has become one of the principal challenges faced by the scientific community in recent years. A significant amount of energy is wasted during mechanical processes due to friction and wear, which can be considered as important generators of power loss and source of noise, vibration and heat transfer effects. As friction reduction leads to costs and energy savings, several tribological studies have been conducted to improve the efficiency of mechanical systems with the major aim of promoting the decrease of the overall energy consumption and pollutant emissions [1–4]. An appealing approach to perform friction and wear evaluations for tribological improvements is to scrutinize the inherent relationship between lubrication regimes and surface topography modifications, such as micro-textures and roughness patterns.

Surface texturing for tribological applications is usually considered with the purpose of reducing friction and/or wear in mechanical components. Surface texturing techniques commonly introduce micro-cavities that locally alter the topography of contact surfaces [5]. The first large utilization of these concepts was for piston ring – cylinder liner assemblies in the 1940s, with the objective of reducing seizure in diesel internal combustion engines (ICEs) [6]. Afterwards, in the 1960s, surface texturing was used with the purpose of reducing adhesion between metal parts in manufacturing operations, such as extrusion and rolling [7]. In the 1990s, probably the largest applications involving surface texturing were based on Laser Surface Texturing (LST) methods, especially for mechanical seals operating under low speed and high load conditions [8]. LST techniques basically consist of a laser beam that promotes the formation of micro-cavities on target surfaces through material ablation. The combination of high laser frequency (up to femtosecond) and large capacity of laser movement and control parameters, permit the fabrication of precise micro-texture geometries, which can act as potential improvers to the lubrication conditions [9–12].

The large utilization of LST in mechanical seals [13–16] is explained by the fact that the hydrodynamic pressure is virtually zero for the parallel and flat surfaces configuration characteristic of such components [17], thus surface textures are designed with the purpose of generating effective load capacity due to the hydrodynamic micro-bearing effect induced by the textures. These surface irregularities generate an asymmetric hydrodynamic pressure distribution caused by the fluid cavitation in the divergent portions of the cavities [3,18,19]. The exploration of these beneficial aspects of surface micro-cavities in boosting the fluid pressure contributed to the disclosure of LST techniques in the last two decades, especially for conformal contacts under

* Corresponding author.
E-mail address: guido.boidi@usp.br (G. Boidi).

https://doi.org/10.1016/j.triboint.2019.02.021
Received 4 July 2018; Received in revised form 12 February 2019; Accepted 13 February 2019
Available online 15 February 2019
0301-679X/

full-film hydrodynamic regime.

In recent years, many results have been reported in the literature showing that the beneficial or detrimental influence of textured surfaces on the tribological performance of lubricated systems strongly depend on the combination of lubrication regime, contact type (conformal or non-conformal) and texture characteristics. Vlădescu et al. [19] studied different texture geometries in reciprocating tests. The author showed that grooves perpendicular to the counter-body movement can be beneficial in boundary and mixed lubrication regimes, although they can present drawbacks under hydrodynamic conditions. This surface configuration can promote reductions in the friction coefficient (COF) of up to 62% as compared to untextured surfaces. Conversely, it was pointed out in this same work that parallel grooves increase the COF.

The tribological effect of textures is also influenced by several other factors, such as test conditions (load, velocity, and temperature), surface materials and lubricant characteristics. The improvement of tribological performance through a specific texture configuration that persists under different experimental conditions is not easily reached. Texture parameters, test conditions and results from different studies were compiled in the comprehensive literature reviews by Sudeep, Tandon and Pandey [20], Gachot et al. [21] and Gropper, Wang and Harvey [22] to support future research projects. Table 1 summarizes the main geometrical features of textures and their beneficial effects under different lubrication regimes adapted from Gachot et al. [21]. As mentioned by the authors, the values presented in the table were taken from different articles and they are no more than indications for texture design and should not be used as rules.

LST has been the object of extensive investigations concerning its beneficial effects in different lubrication regimes and contact conditions; however, some behaviours are still not well understood, such as those encountered in non-compliant elastohydrodynamic point contact conditions [23–26]. Several optimal texture configurations have been proposed to improve the tribological performance of lubricated conformal contacts, such as journal and thrust bearings, mechanical seals and piston ring – liner assembly [1,2,19,22], though the effectiveness of surface features for the reduction of friction and wear has not been widely explored for components with concentrated contacts operating under varying sliding-rolling conditions, such as in gears and cam-tappet applications. In this context, the present contribution is aimed at investigating the effect of three texture configurations fabricated by LST on the frictional behaviour of EHD point contacts under different slide-to-roll ratios (SRR), entrainment velocities and inlet temperatures.

2. Material and methodology

2.1. Ball on disk rig and test parameters

A Mini-Traction Machine (MTM2 – PCS Instruments) was used in the ball-on-disk configuration, as illustrated in Fig. 1. In this experimental configuration, a rotating ball is loaded against a rotating disk, and both disk and ball are moved by different motors in order to achieve a wide variation of sliding-rolling conditions. The slide-to-roll ratio (SRR) parameter is defined as:

$$SRR = 100 \times \frac{U_{Disk} - U_{Ball}}{(U_{Disk} + U_{Ball})/2} = 100 \times \frac{U_s}{U_e} \quad (1)$$

where U_e and U_s are the entrainment and sliding speeds, respectively. SRR ranges from 0% (pure rolling) to 200% (pure sliding).

The ball and disk were placed in a temperature-controlled pot filled with oil, see Fig. 1. The rig permitted variation of SRR and entrainment speed during the test. In this work, the entrainment speed was varied for a given SRR, and each test was repeated three times to ensure statistical reliability. The test parameters used are summarized in Table 2.

The ball was electrically insulated from the disk and the rig could measure the electrical contact resistance (ECR) between the specimens during the test. The amount of solid-to-solid contact could be qualitatively estimated through this technique. In this case, under full-film EHD conditions, the surfaces are not in contact and separate by a lubricant film, therefore the ECR is 100%. Under boundary lubrication the load is totally supported by surface asperities, and hence materials are in contact and ECR is 0%. On the other hand, in the mixed lubrication regime, the load is supported both by the lubricant and asperity contact pressures, hence ECR values range between 0% and 100%. ECR is not a direct measure of the film thickness, nevertheless it is useful to evaluate lubrication regime transitions and lift-off speed, the latter detected when lubricant provides a full separation between the surfaces. This lift-off speed is generally linked to the transition from the mixed to full-film EHD regimes [28].

2.2. Test samples material

Chromium steel (AISI 52100) disks and drilled balls were used for the friction tests. Disks were 46 mm in diameter and 6 mm in thickness, whereas balls were 19.05 mm in diameter. Both disk and balls had smooth surfaces corresponding to S_a = 6 nm and S_q = 20 nm, respectively. Surface textures were applied to the chromium steel disks. Untextured disks (hereafter designated as **NP** – normal production) were used as a reference to be compared with textured ones. A synthetic base oil (PAO 6) was used in all tests. The kinematic viscosity of the oil was measured using an Anton Paar rheometer and the obtained values were 57 mm^2/s, 31 mm^2/s and 9 mm^2/s at 25 °C, 40 °C and 80 °C, respectively.

2.3. Laser surface texturing (LST)

A Titanium-sapphire laser system (PRO 400 seeder amplified by Femtopower Double 10 kHz both from Femtolasers) was used to manufacture the textured disks. The laser had emission centred at 800 nm, pulse length of 30 fs, 10 kHz maximum repetition rate, 200 µJ maximum energy per pulse and linearly polarized emission. The laser beam was focused by a 10X doublet lens producing a focal point of 3.6 µm or 2.4 µm depending on the expansion of the beam before the focusing lens. The sample is moved by a three-axis translator stage (Aerotech

Table 1
Summary of texture geometrical characteristics and effects in different lubrication regimes. Adapted from Gachot et al. [21].

Lubrication Regime			
	Boundary	Mixed	EHD
Effect	Debris trapping Lubricant reservoir	Increase film thickness	Friction reduction
Features depth (µm)	2–15	1–10	< 0.5
Features width (µm)	< contact width	5–100	< contact width
f - Occupied area (%)	–	7–12%	10–20%
Shapes	Pockets/Grooves	Pocket/Grooves/Chevrons	Pocket/Grooves
Directionality	–	Perpendicular	Perpendicular

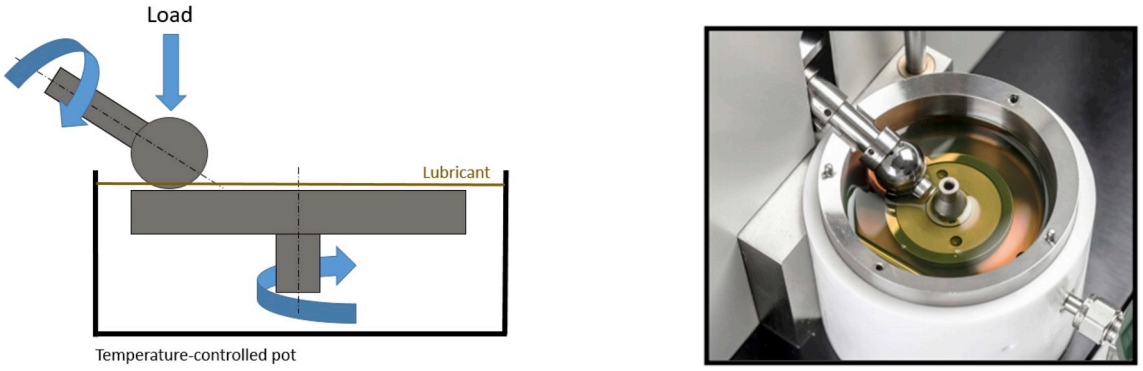

Fig. 1. (a) Schematic representation of MTM rig set-up and (b) real rig, [27].

Table 2
Test parameters used in the MTM rig.

MTM – Ball on disk configuration	
Range of entrainment speed, U_e (mm/s)	2000–10
Slide-to-roll ratio, SRR (%)	5–20 – 50–80 – 100–120 – 150–180
Bath temperature (°C)	25–40 – 80
Maximum Hertzian pressure (GPa)	0.6

ANT130) with G-codes programming.

Micro-dimples (**D**) and radial curved grooves (**RCG**) were manufactured on the MTM steel disks, as shown in Fig. 2. For each type of texture, different dimensional features were obtained by changing laser control parameters, resulting in two texture configurations for grooves and one for dimples. The dimensional and geometrical characteristics of the textures, along with the parameters used in the laser texturing process, are summarized in Table 3. The wear track is constant in the MTM rig; therefore, the uniformity of the test is maintained, even considering the fact that the dimples are further apart as they are further away from the disk centre.

The design selection of the textures was based on the indications reported in the review paper by Gachot [21], whose successful texturing cases for EHD contacts are summarized in Table 1. In this case, the depth was maintained around 0.5 µm for RCG and Dimples configurations. Furthermore, the texture depth was increased (> 1 µm) for the RGC 2 configuration for evaluating the performance of deeper features. The tangential spacing between the textures (~300 µm) was also maintained higher than the contact width (~170 µm) in order to assess the influence of one texture line within the contact and minimize

Table 3
–Geometrical characteristic of disk textures and laser parameters used.

	Radial Curved Grooves		Dimples
Texture profile	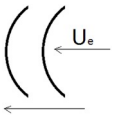 Tangential direction		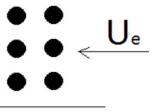 Tangential direction
Texture name	RCG	RCG 2	D
Features width (µm)	25	20	15
Features depth (µm)	0.35	1.35	0.5
Features tangential[a] spacing (µm)	300	300	300
Features transversal spacing (µm)	/	/	10
Features area[b] (%)	12.5	10	1
Features aspect ratio (R = depth/width)	0.01	0.06	0.03
Laser pulse energy (µJ/pulse)	2.8	3.5	1.4
Laser number of overlapped shots	4	5	30
Laser processing speed (mm/s)	9	7	/
Laser spot size (µm)	3.6	3.6	2.4

[a] Tangential direction is the same direction of entrainment speed.
[b] Features area is the texture area over the total coverage area, as adopted in Refs. [21,29,30].

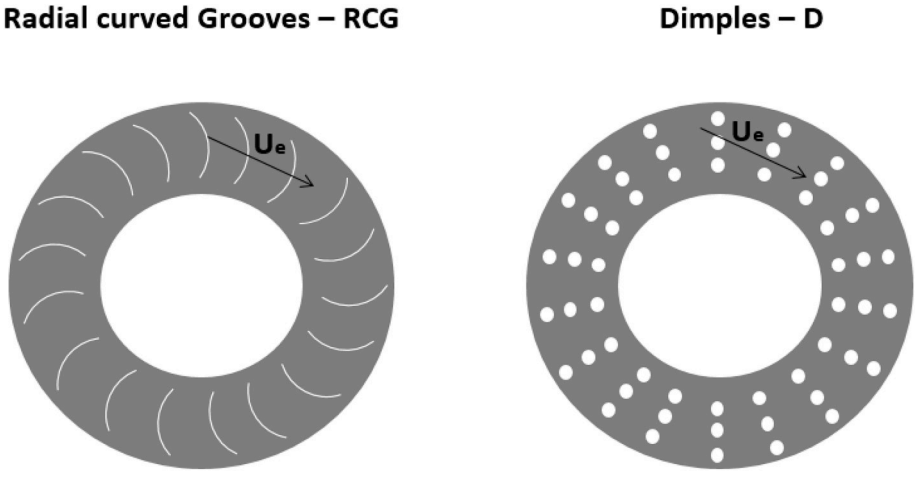

Fig. 2. Schematic representation of texturing configurations manufactured on the MTM disks.

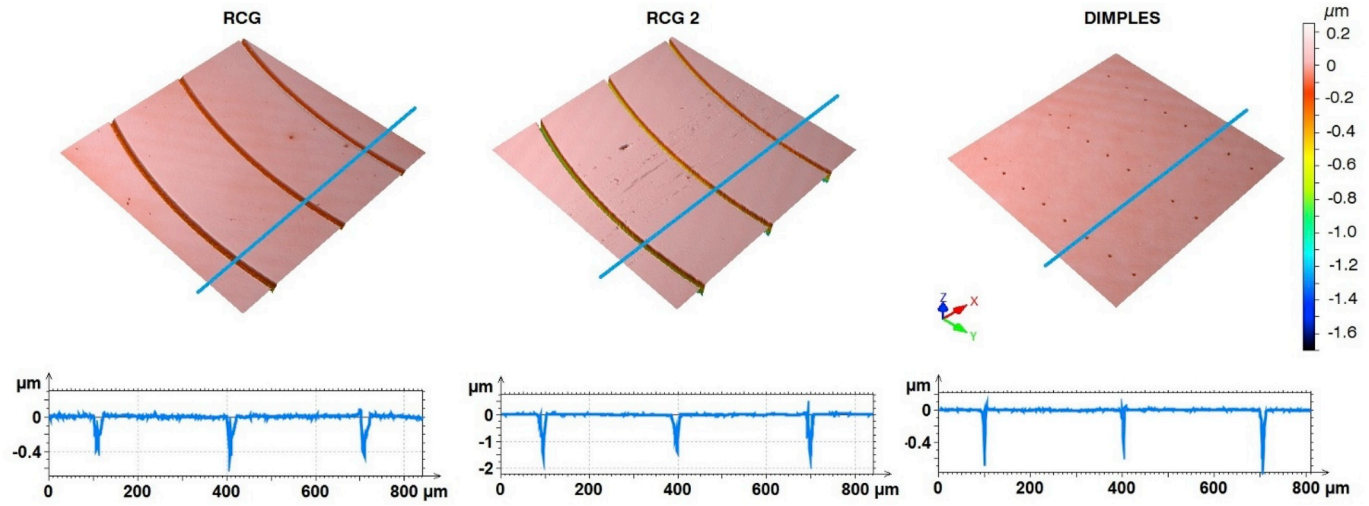

Fig. 3. D surface images (800 µm × 800 µm) and representative 2D profiles of the RCG, RGC2 and Dimples texture configurations.

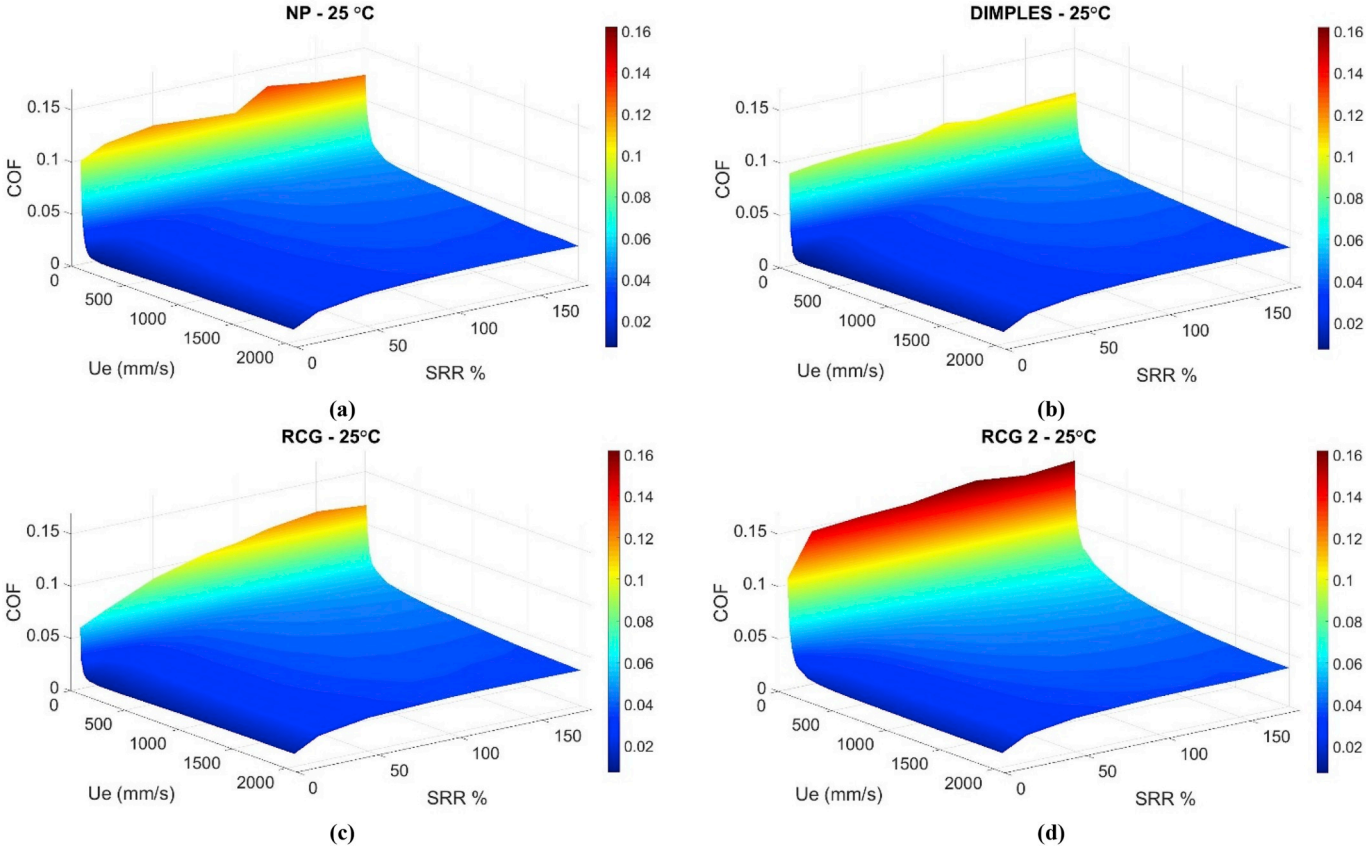

Fig. 4. COF response surface for NP and textured material tested at 25 °C.

potential turbulent effects of the lubricant flow associated with the presence of multiple textures. Finally, the textures width was also designed lower than the contact width to verify the potential application of low-density texturing in real applications.

3. Results

The 3D surface topographies and representative 2D profiles of the three texture configurations investigated in the present work are shown in Fig. 3.

The coefficient of friction (COF) can be traced as a function of the sliding speed (Stribeck curves) or SRR (traction curves). By combining the Stribeck and traction curves made it possible to obtain a response surface, or traction map, in the form of COF x U_e x SRR. In the following, the obtained friction results for the different testing temperatures (25 °C, 40 °C, 80 °C) and maximum Hertzian pressure (0.6 GPa) considered in this contribution are discussed in details through the mentioned traction maps.

3.1. Tribological test at 25 °C

As can be seen in Fig. 4, COF response surfaces are displayed with

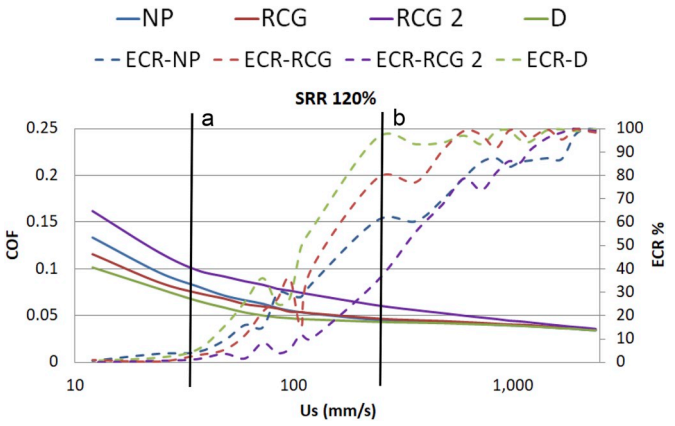

Fig. 5. COF x Us (left vertical axis) and ECR x Us (right vertical axis) for SRR 120%, NP and textured materials tested at 25 °C.

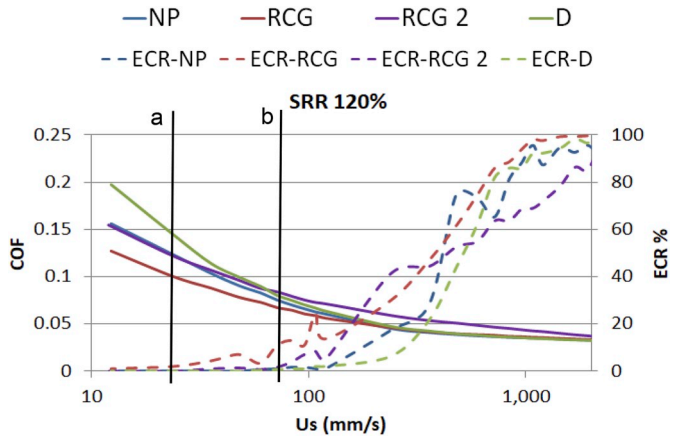

Fig. 7. COF x Us (left vertical axis) and ECR x Us (right vertical axis) (SRR 120%) of NP and textured materials tested at 40 °C.

the same scale and colour map to permit better comparisons. Significant differences can be noticed at low entrainment speed (U_e), especially between NP and RCG cases (see Fig. 4a and c).

For SRRs over 100% (50% of sliding) the results for the four configurations presented similar trends, as can be seen in Fig. 5. COF results were plotted jointly with ECR values to better understand the influence of textures on the transition between lubrication regimes. Boundary and full-film EHD regimes were discriminated by ECR of 0% and 100%, respectively, as explained in Section 2.1. Line 'b' in Fig. 5 shows that the dimples (D) configuration promoted a decrease in the lift-off speed compared to the untextured surface (NP). This behaviour benefited full-film EHD condition and, consequently, dimple textured surface presented lower COF.

Furthermore, RCG configuration also seemed to decrease lift-off speed compared to NP, leading to an intermediate condition between NP and Dimples. NP and RCG 2 configuration presented higher lift-off speed and generally operated under mixed and boundary lubrication conditions. The transition between mixed and boundary regimes took place approximately at the same speed for all configurations, as can be visualized through the vertical line 'a' in Fig. 5.

3.2. Tribological test at 40 °C

Similarly, for the testing temperature of 40 °C, significant differences can be noticed at low entrainment speed (U_e), especially between NP and Dimples configurations, as shown in Fig. 6a and b.

COF results for SRR 120% were also plotted jointly with ECR values

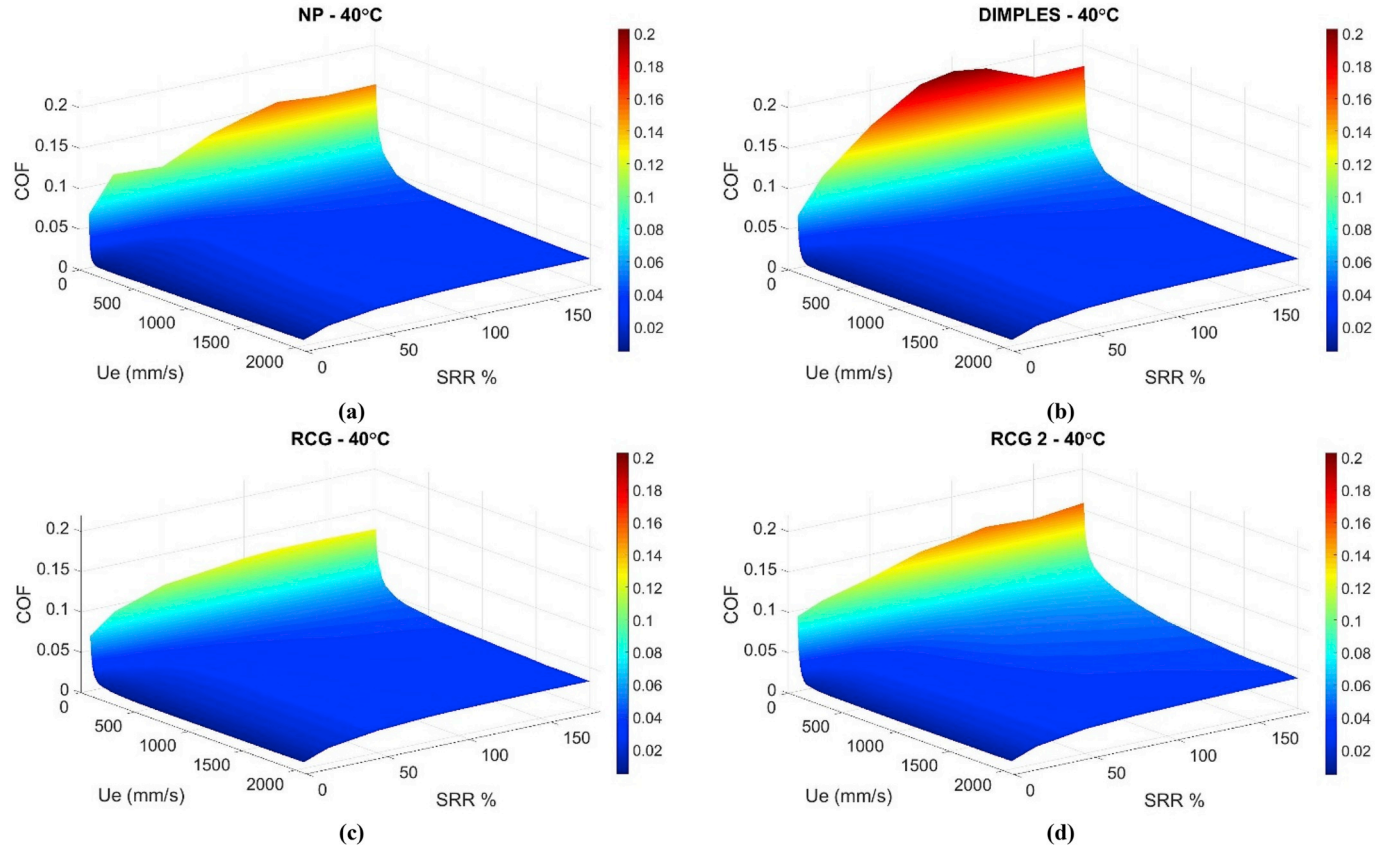

Fig. 6. COF response surface for NP and textured material tested at 40 °C.

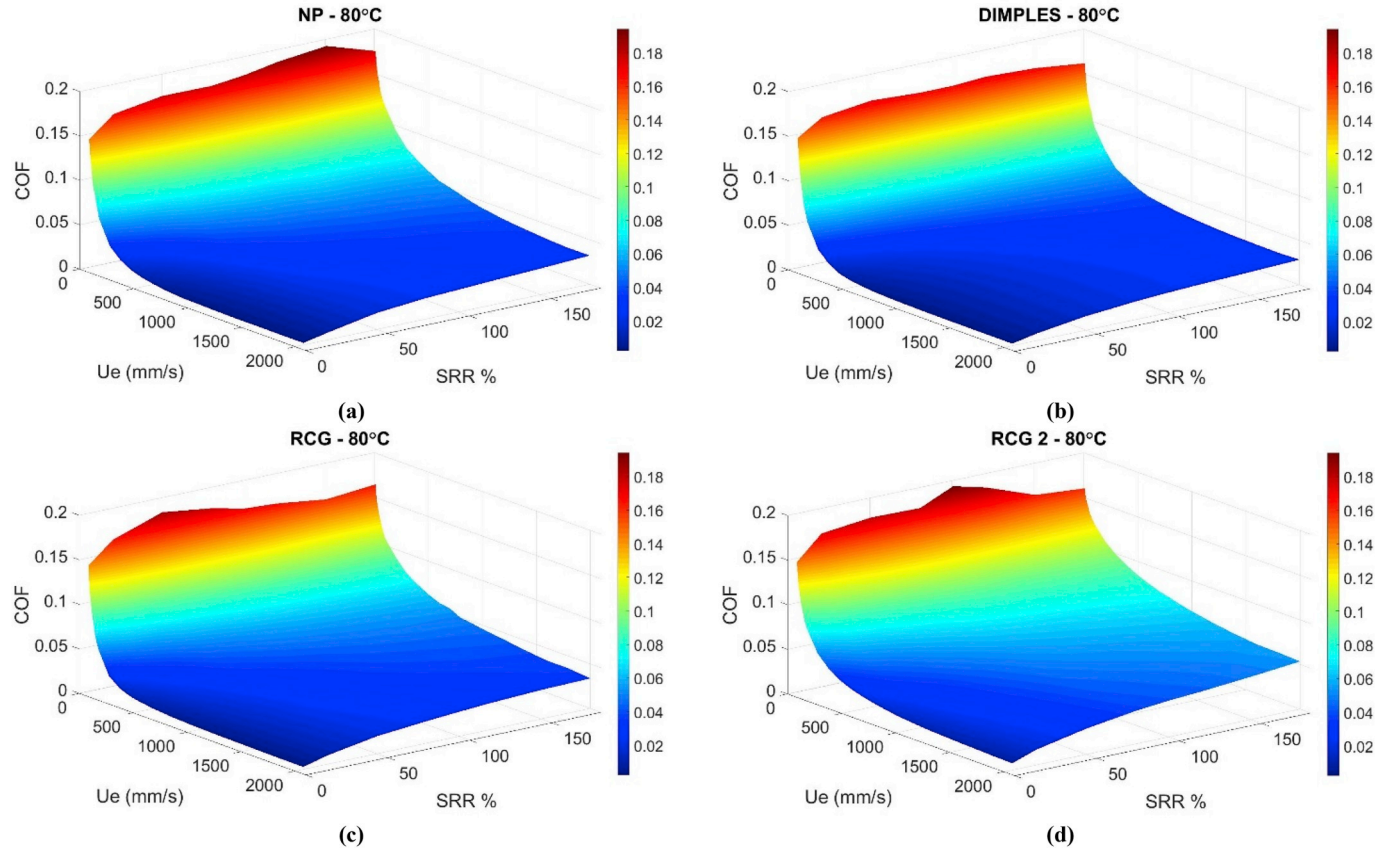

Fig. 8. COF response surface for NP and textured material tested at 80 °C.

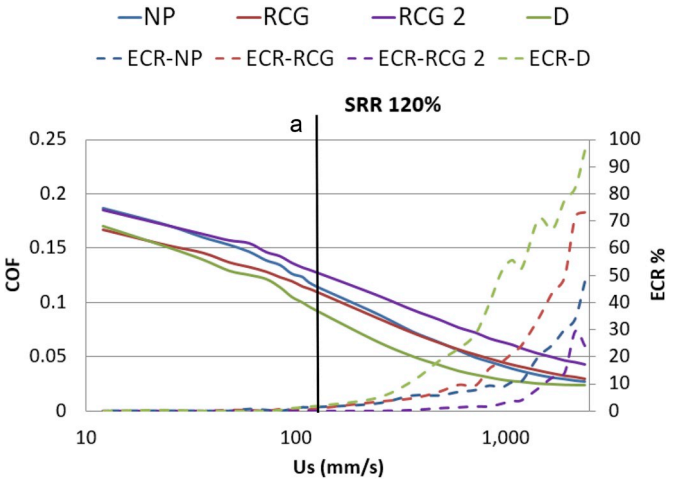

Fig. 9. COF x Us (left vertical axis) and ECR x Us (right vertical axis) (SRR 120%) of NP and textured materials tested at 80 °C.

in Fig. 7. The increase of temperature (40 °C) led to viscosity decrease and, consequently, only Dimples and RCG configurations operated under full-film EHD conditions for a reduced range of sliding velocities. Therefore, in these cases, tests were carried out mainly in mixed and boundary lubrication regimes.

RCG promoted friction reduction, especially over SRR 100% and low speeds. The transition between mixed and boundary regimes for RCG occurred at lower speeds compared to the other configurations (see vertical line 'a' and 'b', respectively, in Fig. 7). On the contrary, Dimples configuration operated only in boundary lubrication at low speeds, showing higher COF than RCG under similar conditions.

3.3. Tribological test at 80 °C

COF response surfaces for the testing temperature of 80 °C are displayed in Fig. 8, showing again significant differences at low entrainment speeds.

Dimples configuration was the only one that still favoured full-film EHD regime for low viscosity tests (80 °C), presenting elevated ECR values around 80%–100% only at high speeds (see Fig. 9). Conversely, RCG, NP and RCG 2 practically did not reach lift-off speed, thus concluding that the experiments for these configurations were conducted mostly under mixed and boundary lubrication conditions.

The transition from boundary to mixed lubrication regimes occurred for similar sliding speeds for all texture configurations (see vertical line 'a' in Fig. 9). Dimples, besides providing a complete separation between the contacting surfaces during the initial stages of the test (high speeds), also promoted a slight friction reduction under boundary and mixed lubrication conditions.

3.4. Wear results

In order to evaluate the possible occurrence of texture geometry modifications due to wear, surface topography measurements were carried out over a wear track region of the dimple textured sample. As can be observed in Fig. 10b, the surface ridges within the wear track did not significantly affect the dimples geometry. Furthermore, the roughness parameters remained unchanged and a significant wear mark could not be measured on the ball surface after the test. Similar results were verified for the other texture configurations.

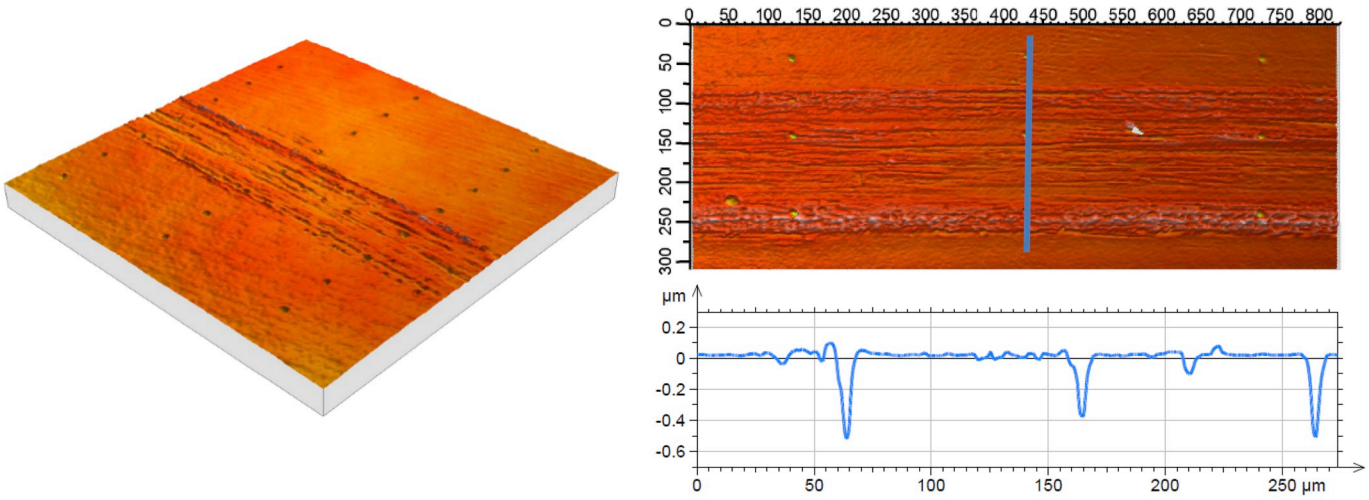

(a) (b)

Fig. 10. (a) 3D surface image (800 µm × 800 µm) showing the wear track on dimple textured disk. (b) Detailed view of the wear track and representative 2D profile along a row of dimples.

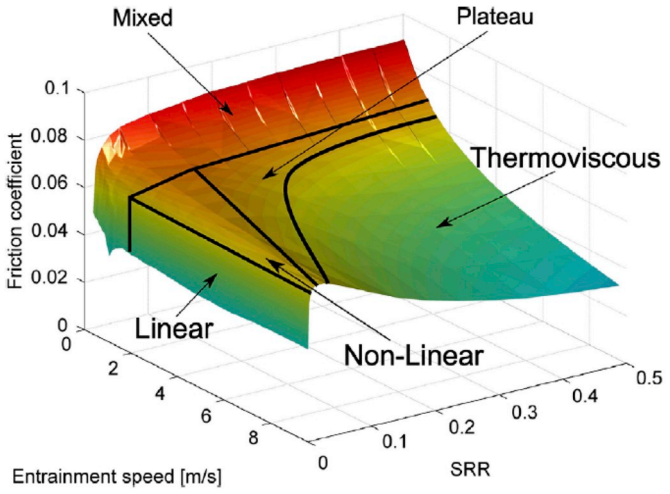

Fig. 11. COF response surface showing the EHD friction regimes [32]. Marcus Björling from Luleå University of technology and Elsevier kindly gave the permission to use this figure (License Number 4514230079050), which was previously published by Marcus Björling in Tribology International Journal [32].

4. Discussion

4.1. Texture effect in different lubrication regimes

Different friction regimes can be encountered in elastohydrodynamic point contacts, as highlighted in Ref. [31]. Four different regions could be discriminated based on thermal effects, limiting shear stress and shear thinning behaviour, as illustrated in Fig. 11.

In **linear regime**, the friction increases linearly with SRR, thus shear stress is proportional to share rate, according to Newtonian viscous behaviour. The increase of SRR leads to a **non-linear region**, in which shear thinning and limiting shear stress affect the friction behaviour. The increase of sliding can also promote friction decrease due to thermal and shear thinning effects in **thermoviscous regime**, as proved by Habchi [31]. Finally, in **plateau regime**, friction remains almost constant and limiting shear stress in lubricant is the leading mechanism. However, as pointed out by Habchi [31] not all regimes are always encountered in conventional traction curves. For instance, in the present work, the non-linear and the plateau regimes could be identified (Figs. 4, 6 and 8), whereas the linear and thermoviscous regimes did not appear clearly. The last two regimes are more likely to occur at high entrainment speeds, which are not easily reached during traction experiments.

It is difficult to determine in which friction regime the texture configurations considered in the present work promoted COF reduction by simple inspection of Figs. 4, 6 and 8. Thus, the COF response surfaces of the textured samples shown in Section 3 were subtracted from the NP ones to better evaluate the beneficial or detrimental effects promoted by the textures. The difference COF response surfaces (Delta) were defined as:

$$Delta = COF_{texture} - COF_{NP} \quad (2)$$

where negative values of Delta represent COF reduction. In Fig. 12, the entrainment speed U_e was plotted in reverse direction compared to Figs. 4, 6 and 8, being that significant difference in COF were encountered at low entrainment speeds (mixed and boundary lubrication regimes).

According to Fig. 12, at 25 °C similar friction results were observed in the plateau and non-linear regions for all texture configurations. As viscosity decreased (40 °C), some difference could be encountered in plateau regime, whereas at lower viscosity conditions (80 °C) the difference between NP and textured samples became more relevant (see Fig. 12c). This trend can be explained by the fact that the plateau and non-linear friction regions are governed by the limiting shear stress behaviour of the lubricant, and that the increment of test temperature led to a combined drop in viscosity, limiting shear strength and pressure viscosity coefficient, as reported by Larsson [33]. For this reason, some texture configurations investigated in this work, especially Dimples and RCG, seem to act positively on reducing friction in the plateau regime region under harsher lubrication conditions characterized by low lubricant viscosity and shear stress limit.

Summarizing, Fig. 12 shows that the textured surfaces significantly affected the frictional behaviour in the boundary and mixed lubrication regimes, especially at low entrainment speeds and high SRR values. Similar results were also highlighted by Mourier [10]. Furthermore, the decrease of viscosity and shear stress limit at higher temperatures also influenced the texture tribological performance in full-film EHD regime, especially in the plateau friction region. This latter result for the full-film EHD regime is in agreement with the results reported by Wang et al. [34] and Braun et al. [35], which stated that texture tribological

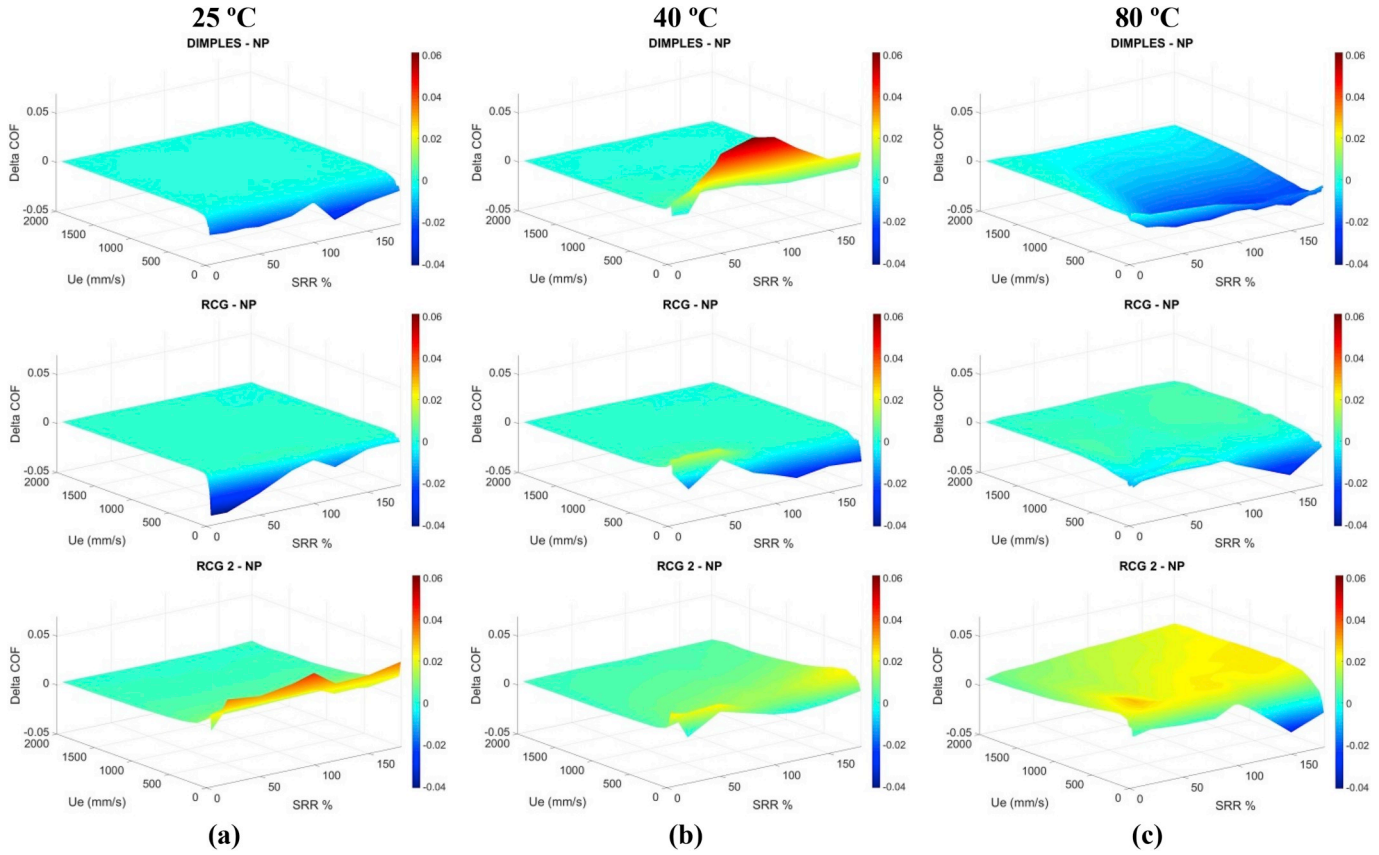

Fig. 12. Delta COF response surface between NP and Dimples, RCG, RCG 2 textured material tested at (a) 25 °C, (b) 40 °C and (c) 80 °C.

efficiency is straight related to viscosity and feature geometry. A texture configuration could promote friction reductions at a certain viscosity value, however it could bring detrimental effect in other viscosity conditions.

4.2. Texture geometry effect

Dimples configuration improved the tribological results in full-film EHD regime. As shown in Fig. 5, dimple textured surface decreased lift-off speed at high viscosity conditions (25 °C), promoting a wider range of speeds operating under full-film EHD and lower COF. This behaviour could also be encountered in low viscosity tests (80 °C), being that dimples is the unique configuration that still promoted full-film EHD conditions at high temperature (see Fig. 9). The beneficial effect of dimples could be associated with their shallow depth configuration (~0.5 μm), as reported in Table 1. Mourier et al. [10] explained that shallow features could induce a film thickness increase in EHD lubrication due to local pressure and viscosity increment. Besides that, Krupka [26] measured local film thickness increment close to surface dimples, caused by viscosity increase within the micro-cavities.

Comparing the dimensions of the texture configurations that resulted in COF reduction, RCG was shallower and covered much more area than Dimples (see Table 3). Despite this, Dimples configuration produced better results probably because of the presence of several micro-cavities, which are more efficient at entrapping lubricant than a single feature (RCG).

Dimples also promoted friction reduction in boundary and mixed lubrication regimes, as shown in Fig. 9. The tribological performance of dimple textured surfaces in these regimes is straight related to viscosity and geometrical aspects, as reported by Wang et al. [34]. The authors showed that under boundary lubrication conditions, shallow dimples reduced friction probably due to squeeze effect [34], otherwise other configuration increased friction compared to an untextured material.

On the other hand, dimples configuration resulted in detrimental effect compared to NP material at 40 °C (see Fig. 7), where the mixed lubrication was predominant. This configuration presented lower depth and area coverage than values presented in Table 1 for mixed regime.

RCG configuration had the best performance in reducing friction at intermediate viscosity condition (40 °C), where mixed lubrication regime was predominant (Fig. 7). For instance, RCG texture parameters were designed to improve efficiency under mixed lubrication conditions and they were similar to those reported in Table 1 for the same lubrication regime, except for the feature depth, which was lower than 1 μm. RCG favoured the mixed lubrication for a wider range of speeds at 40 °C, moving the transition from boundary to mixed regimes to lower speed values (see vertical line 'a' in Fig. 7). Furthermore, RCG configuration also promoted friction reduction at 25 °C and 80 °C, probably due to its shallow depth.

RCG 2 performed worse than NP and RCG in all conditions, showing that texture depth is a critical geometrical parameter that should be considered for the texture design of non-conformal contacts. As reported by Mourier [10], deep features as RCG 2 could lead to a local pressure reduction and, consequently, a viscosity drop. In this case, the lubricant could not provide a sufficient film thickness to completely separate the contacting surface (see Fig. 5).

To conclude, this work aimed at evaluating the tribological performance of textured surfaces fabricated by LST in EHD point contacts under different sliding-rolling conditions and inlet temperatures, as well as to understand the underlying mechanisms governing the influence of textures on the lubrication behaviour of concentrated contacts. This work, besides providing a methodology to evaluate the friction response of EHD point contacts with textured surfaces in different lubrication regimes, could also help to support the design of surface textures for friction reduction with focus on practical engineering applications.

5. Conclusion

The influence of three texture configurations (2 radial curved grooves and 1 micro-dimple textured surfaces) fabricated by LST technique on the tribological performance of EHD point contacts under different sliding-rolling conditions, entrainment velocities and inlet temperatures was experimentally investigated through a series of ball-on-disk tests conducted in the MTM-2 tribometer. The following conclusions could be drawn from this study:

- The texture configurations investigated promoted significant effects in boundary and mixed lubrication regimes (low entrainment speeds), and also affected the full-film EHD regime at higher temperatures due to the decrease in lubricant viscosity;
- For non-conformal contacts, the tribological performance of textured samples are strongly related to the texture depth. Shallow textures (RCG and Dimples) promoted friction reduction, whereas deeper cavities (RCG 2) yielded to detrimental results;
- Dimples promoted best results in boundary and full-film EHD lubrication regimes. At 25 °C, this configuration induced full-film conditions for a larger range of speeds, whereas at 80 °C it favoured friction reduction in mixed/boundary regimes, beside boosting an initial full-film condition;
- RCG yielded to friction reduction under mixed lubrication conditions, moving the transition from boundary to mixed regimes to lower speeds, especially for intermediate lubricant viscosity (40 °C).

Acknowledgments

The authors recognize the Funding Agency for Research in São Paulo State, Brazil (FAPESP grant N. 2013/26113-6 and 2017/21151-8) and the National Council for Scientific and Technological Development, Brazil (CNPq) for their generous financial support. The authors also thank Marcus Björling from Luleå University of technology and Elsevier for the kind permission of using Fig. 11, previously published in Ref. [32] (License Number 4514230079050).

References

[1] Priest M, Taylor CM. Automobile engine tribology—approaching the surface. Wear 2000;241:193–203. https://doi.org/10.1016/S0043-1648(00)00375-6.
[2] Ryk G, Etsion I. Testing piston rings with partial laser surface texturing for friction reduction. Wear 2006;261:792–6. https://doi.org/10.1016/j.wear.2006.01.031.
[3] Vlădescu SC, Olver AV, Pegg IG, Reddyhoff T. Combined friction and wear reduction in a reciprocating contact through laser surface texturing. Wear 2016;358–359:51–61. https://doi.org/10.1016/j.wear.2016.03.035.
[4] Ronen A, Etsion I, Kligerman Y. Friction-reducing surface-texturing in reciprocating automotive components. Tribol. Trans. 2001;44:359–66. https://doi.org/10.1080/10402000108982468.
[5] Hamilton DB, Walowit JA, Allen CM. A theory of lubrication by micro- irregularities. J. Basic Eng. 1966;88:177–85. https://doi.org/10.1017/CBO9781107415324.004.
[6] Spencer A. Optimizing surface texture for combustion engine cylinder liners. 2010.
[7] Wennber JL, Turkovich BF, Roubik JR, Boulger FW, Hahn RS, Smith PA. Review of metal processing literature. J. Eng. Ind. 1965:85–96.
[8] Ranjan R, Lambeth DN, Tromel M, Goglia P, Li Y. Laser texturing for low-flying-height media. J. Appl. Phys 1991;69:5745–7. https://doi.org/10.1063/1.347908.
[9] Pettersson U, Jacobson S. Influence of surface texture on boundary lubricated sliding contacts. Tribol. Int. 2003;36:857–64. https://doi.org/10.1016/S0301-679X(03)00104-X.
[10] Mourier L, Mazuyer D, Lubrecht AA, Donnet C. Transient increase of film thickness in micro-textured EHL contacts. Tribol. Int. 2006;39:1745–56. https://doi.org/10.1016/j.triboint.2006.02.037.
[11] Kovalchenko A, Ajayi O, Erdemir A, Fenske G, Etsion I. The effect of laser texturing of steel surfaces and speed-load parameters on the transition of lubrication regime from boundary to hydrodynamic. Tribol. Trans. 2004;47:299–307. https://doi.org/10.1080/05698190490440902.
[12] Kovalchenko A, Ajayi O, Erdemir A, Fenske G, Etsion I. The effect of laser surface texturing on transitions in lubrication regimes during unidirectional sliding contact. Tribol. Int. 2005;38:219–25. https://doi.org/10.1016/j.triboint.2004.08.004.
[13] Brizmer V, Kligerman Y, Etsion I. A laser surface textured parallel thrust bearing. Tribol. Trans. 2003;46:397–403. https://doi.org/10.1080/10402000308982643.
[14] Etsion I, Halperin G. A laser surface textured hydrostatic mechanical seal. Tribol. Trans. 2002;45:430–4. https://doi.org/10.1080/10402000208982570.
[15] Ahmed A, Masjuki HH, Varman M, Kalam MA, Habibullah M, Al Mahmud KAH. An overview of geometrical parameters of surface texturing for piston/cylinder assembly and mechanical seals. Meccanica 2015:9–23. https://doi.org/10.1007/s11012-015-0180-6.
[16] Etsion I, Kligerman Y, Halperin G. Analytical and experimental investigation of laser- textured mechanical seal faces. Tribol. Trans. 2008;42:511–6. https://doi.org/10.1080/10402009908982248.
[17] Hamrock BJ, Schmid SR. Fundamental of fluid film lubrication. second ed. 2004.
[18] Qui Y, Khonsari MM. On the prediction of cavitation in dimples using a mass-conservative algorithm. J. Tribol. 2009;131. https://doi.org/10.1115/1.3176994.
[19] Vlădescu SC, Olver AV, Pegg IG, Reddyhoff T. The effects of surface texture in reciprocating contacts - an experimental study. Tribol. Int. 2015;82:28–42. https://doi.org/10.1016/j.triboint.2014.09.015.
[20] Sudeep U, Tandon N, Pandey RK. Performance of lubricated rolling/sliding concentrated contacts with surface textures: a review. J. Tribol. 2015;137:31501. https://doi.org/10.1115/1.4029770.
[21] Gachot C, Rosenkranz A, Hsu SM, Costa HL. A critical assessment of surface texturing for friction and wear improvement. Wear 2017;372–373:21–41. https://doi.org/10.1016/j.wear.2016.11.020.
[22] Gropper D, Wang L, Harvey TJ. Tribology International Hydrodynamic lubrication of textured surfaces : a review of modeling techniques and key fi ndings vol.94. 2016. p. 509–29. https://doi.org/10.1016/j.triboint.2015.10.009.
[23] Rosenkranz A, Szurdak A, Gachot C, Hirt G, Mücklich F. Friction reduction under mixed and full film EHL induced by hot micro-coined surface patterns. Tribol. Int. 2016;95:290–7. https://doi.org/10.1016/j.triboint.2015.11.035.
[24] Gao L, De Boer G, Hewson R. The role of micro-cavitation on EHL: a study using a multiscale mass conserving approach. Tribol. Int. 2015;90:324–31. https://doi.org/10.1016/j.triboint.2015.04.005.
[25] Mourier L, Mazuyer D, Ninove FP, Lubrecht AA. Lubrication mechanisms with laser-surface-textured surfaces in elastohydrodynamic regime. Proc. Inst. Mech. Eng. Part. J. J. Eng. Tribol. 2010;224:697–711. https://doi.org/10.1243/13506501JET771.
[26] Krupka I, Hartl M, Zimmerman M, Houska P, Jang S. Effect of surface texturing on elastohydrodynamically lubricated contact under transient speed conditions. Tribol. Int. 2011;44:1144–50. https://doi.org/10.1016/j.triboint.2011.05.005.
[27] PCS Instruments. MTM2 mini-traction machine. http://pcs-instruments.com/wp-content/uploads/2017/01/MTM2-brochure-2017-Publisher-version-1.pdf; 2017.
[28] Heemskerk RS, Vermeiren KN, Dolfsma H. Measurement of lubrication condition in rolling element bearings. ASLE. Trans. 1982;25:519–27. https://doi.org/10.1080/05698198208983121.
[29] Schneider J, Braun D, Greiner C. Laser textured surfaces for mixed Lubrication : influence of aspect ratio , textured area and dimple arrangement. 2017. https://doi.org/10.3390/lubricants5030032.
[30] Youqiang X, Jianxin D, Xiuting F, Sheng Y. Effect of laser surface texturing on Si 3 N 4/TiC ceramic sliding against steel under dry friction. Mater. Des. 2013;52:234–45. https://doi.org/10.1016/j.matdes.2013.05.077.
[31] Habchi W, Bair S, Vergne P. On friction regimes in quantitative elastohydrodynamics. Tribol. Int. 2013;58:107–17. https://doi.org/10.1016/j.triboint.2012.10.005.
[32] Björling M, Habchi W, Bair S, Larsson R, Marklund P. Towards the true prediction of EHL friction. Tribol. Int. 2013;66:19–26. https://doi.org/10.1016/j.triboint.2013.04.008.
[33] Larsson R, Larsson PO, Eriksson E, Sjöberg M, Höglund E. Lubricant properties for input to hydrodynamic and elastohydrodynamic lubrication analyses. Proc .Inst. Mech. Eng. Part. J. J. Eng. Tribol. 2000;214:17–27. https://doi.org/10.1243/1350650001542981.
[34] Wang X, Zhang H, Hsu SM. The Effects of dimple size and depth on friction reduction under boundary lubrication pressure. 2007. p. 24–6.
[35] Braun D, Greiner C, Schneider J, Gumbsch P. Efficiency of laser surface texturing in the reduction of friction under mixed lubrication. Tribol. Int. 2014;77:142–7. https://doi.org/10.1016/j.triboint.2014.04.012.